Ann. Geophys., 29, 221–227, 2011
www.ann-geophys.net/29/221/2011/
doi:10.5194/angeo-29-221-2011

Annales Geophysicae

Performance of the HOMME dynamical core in the aqua-planet configuration of NCAR CAM4: equatorial waves

S. K. Mishra[1,2], **M. A. Taylor**[3], **R. D. Nair**[2], **H. M. Tufo**[1,2], **and J. J. Tribbia**[2]

[1]Department of Computer Science, University of Colorado, Boulder, CO, USA
[2]National Center for Atmospheric Research (NCAR), Boulder, CO, USA
[3]Sandia National Laboratories, Albuquerque, NM, USA

Received: 8 October 2010 – Revised: 10 November 2010 – Accepted: 17 November 2010 – Published: 2 February 2011

Abstract. A new atmospheric dynamical core, named the High Order Method Modeling Environment (HOMME), has been recently included in the NCAR-Community Climate System Model version 4 (CCSM4). It is a petascale capable high-order element-based conservative dynamical core developed on a cubed-sphere grid. We have examined the model simulations with HOMME using the aqua-planet mode of CAM4 (atmospheric component of CCSM4) and evaluated its performance in simulating the equatorial waves, considered a crucial element of climate variability. For this we compared the results with two other established models in CAM4 framework, which are the finite-volume (FV) and Eulerian spectral (EUL) dynamical cores. Although the gross features seem to be comparable, important differences have been found among the three dynamical cores. The phase speed of Kelvin waves in HOMME is faster and more satisfactory than those in FV and EUL. The higher phase speed is attributed to an increased large-scale precipitation in the upper troposphere and a more top-heavy heating structure. The variance of the $n = 1$ equatorial Rossby waves is underestimated by all three of them, but comparatively HOMME simulations are more reasonable. For the $n = 0$ eastward inertio-gravity waves, the variances are weak and phase speeds are too slow, scaled to shallow equivalent depths. However, the variance in HOMME is relatively more compared to the two other dynamical cores. The mixed Rossby-gravity waves are feeble in all the three cases. In summary, model simulations using HOMME are reasonably good, with some improvement relative to FV and EUL in capturing some of the important characteristics associated with equatorial waves.

Keywords. Meteorology and atmospheric dynamics (Tropical meteorology)

Correspondence to: S. K. Mishra
(saroj@ucar.edu)

1 Introduction

The future evolution of the Community Climate System Model (CCSM) into an Earth system model will require a highly scalable and accurate conservative formulation of the dynamics of the atmosphere. Conservative formulation of the primitive equations is highly desirable for long-term climate simulation. Accurate numerical schemes are essential to ensure high-fidelity simulations capable of capturing the convective dynamics in the atmosphere and its contribution to the global hydrological cycle. Scalable performance is necessary to efficiently exploit the massively-parallel petascale systems that will dominate high-performance computing for the foreseeable future (Nair and Tufo, 2007; Taylor et al., 2008; Nair et al., 2009). The High Order Method Modeling Environment (HOMME) is a framework developed at NCAR (Dennis et al., 2005; Taylor et al., 2007, 2008; Taylor, 2010) to investigate using high-order element-based methods to build scalable, accurate and conservative atmospheric general circulation models (AGCM). The primary object of HOMME project is to provide the atmospheric science community a framework for building the next generation of AGCMs based on high-order numerical methods that efficiently scale to hundred-of-thousands of processors, achieve scientifically useful integration rates, provide monotonic and mass conserving transport of multiple species, and can easily be coupled to community physics packages (Taylor, 2010).

Recently, HOMME has been integrated into the Community Atmosphere Model (CAM), the atmospheric component of the CCSM. Initial HOMME simulations have been completed, using the CAM4 physics (also called as Track 1 physics, see Neale et al., 2010) in the aqua-planet configuration. In this paper, we examine the equatorial waves which are major transient features and are important for climate variability. Since the true climate of an aqua-planet is

Published by Copernicus Publications on behalf of the European Geosciences Union.

AnGeo Communicates

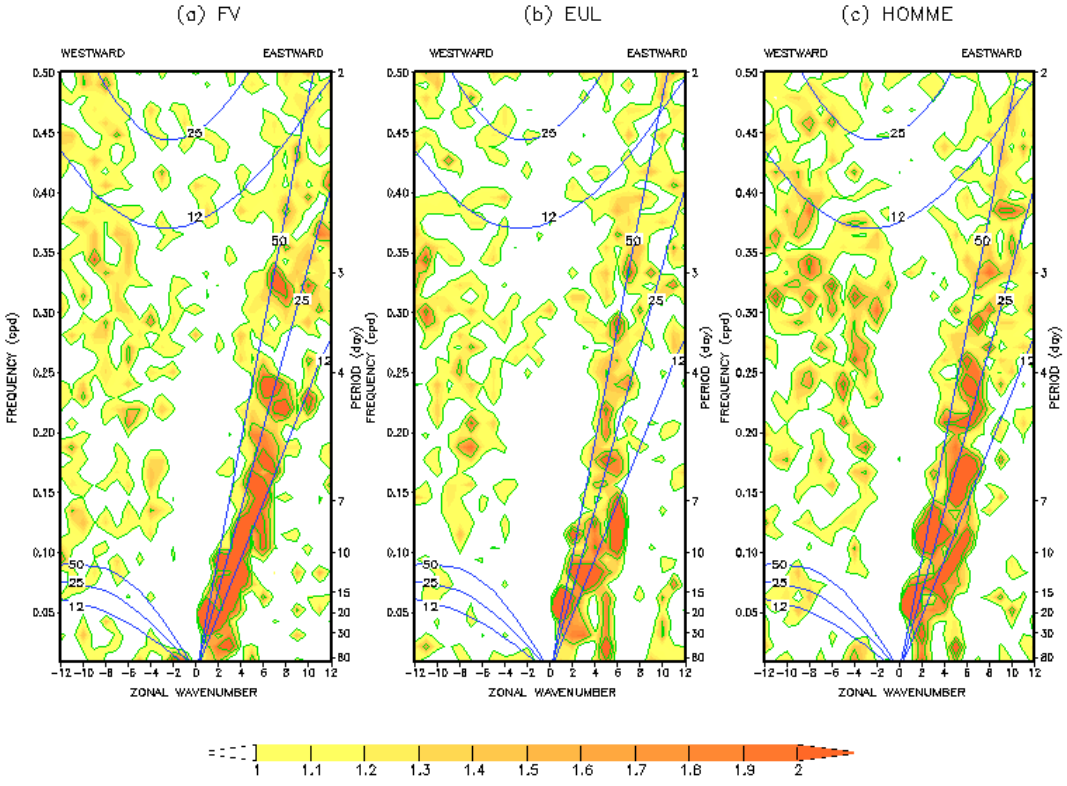

Fig. 1. The symmetric component of the frequency-wavenumber distribution of OLR averaged between 15° S and 15° N is shown, **(a)** FV, **(b)** EUL, and **(c)** HOMME. (Wheller and Kiladis, 1999, technique is used).

unknown, in order to assess the performance of HOMME, the comparisons have been made with the other two established dynamical cores of NCAR CAM4 i.e. Finite Volume (FV) and Eulerian (EUL).

2 Model and simulation details

The Community Atmosphere Model version 4 (CAM4) is the sixth generation atmospheric general circulation models (AGCMs) developed by the atmospheric modeling community in collaboration with the National Center for Atmospheric Research (NCAR). For a detail description of CAM4 see Neale et al. (2010). CAM4 has been designed to produce simulations with reasonable accuracy for various dynamical cores and horizontal resolutions. For this study, FV, EUL, and HOMME dynamical cores were used at 1° equivalent resolutions in horizontal and 26 levels in vertical. All three dynamical cores use the same physical parameterization package. All simulations were performed in the aqua-planet configuration of CAM4 based on standard experiments set by Neale and Hoskins (2000). The initial condition for all simulations was from a previous aqua-planet simulation. All the simulations were performed for 24 months, and the last 18 months were considered for the analysis.

HOMME uses the continuous Galerkin spectral element method (Taylor et al., 2010). This method is designed for fully unstructured quadrilateral meshes. The current configurations in CAM are based on the cubed-sphere grid (Taylor et al., 2007, 2008; Bhanot et al., 2008; Nair et al., 2009). Spectral elements are a kind of a continuous Galerkin h-p finite element method (Karniadakis and Sherwin, 1999; Canuto et al., 2007), where h is the number of elements and p the polynomial order. The method uses p-order polynomials to represent the prognostic variables inside each element. The cubed-sphere grid consists of elements with boundaries defined by an equiangular genomic grid (Nair et al., 2005) and each elements has $(p+1)\times(p+1)$ Gauss-Legendre-Lobatto quadrature points. The main motivation for the inclusion of HOMME is to improve the scalability of the CAM by introducing quasi-uniform grids, which require no polar filters (Taylor et al., 2008). HOMME is the first dynamical core in CAM, which locally conserves energy in addition to mass and two-dimensional potential vorticity (Taylor, 2010). HOMME represents a large change in the horizontal grid as compared to the other dynamical cores in CAM. Almost all other aspects of HOMME are based on a combination of well-tested approaches from the Eulerian and FV dynamical cores. For tracer advection, HOMME is modeled as closely as possible to the FV dynamical core. It

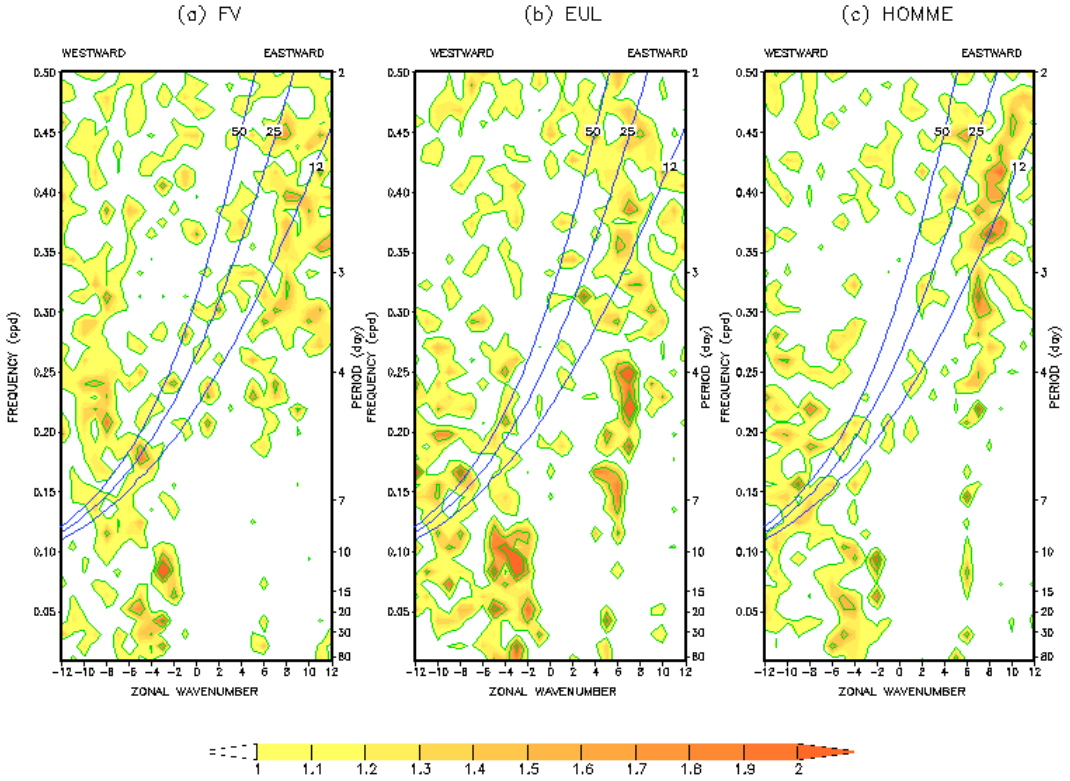

Fig. 2. The antisymmetric component of the frequency-wavenumber distribution of OLR averaged between 15° S and 15° N is shown, **(a)** FV, **(b)** EUL, and **(c)** HOMME. (Wheller and Kiladis, 1999, technique is used).

relies on same conservation form of the transport equation in horizontal, and employs the same vertically-Lagrangian discretization. The HOMME dynamics are modeled similar to Eulerian dynamical core. They share the same vertical coordinate, vertical discretization, hyper-viscosity based horizontal diffusion, top-of-model dissipation, and solve the same moist hydrostatic equations. The main differences are that HOMME advects the surface pressure instead of its logarithm (in order to conserve mass and energy), and HOMME uses the vector-invariant form of the momentum equation instead of the vorticity-divergence formulation. The time stepping in HOMME is a form of dynamics/tracer/physics subcycling, achieved through the use of N-stage 2nd order accurate Runge-Kutta methods. This method allows for a gravity-wave based Courant-Friedrichs-Lewy (CFL) number close to $N-1$, (normalized so that the largest stable time step of the Robert filtered leapfrog method has a CFL number of 1.0). The value of N is chosen large enough so that the dynamics will be stable at the same time step used by the tracer advection scheme. To determine N, we first note that the tracer advection scheme uses a less efficient (in terms of maximum CFL) strong stability preserving Runge-Kutta method. It is stable at an advective CFL number of 1.4. Let u_0 be a maximum wind speed and c_0 be the maximum gravity wave speed. The gravity wave and advective CFL conditions are:

$$\Delta t \leq (N-1)\Delta x/c_0, \Delta t \leq 1.4\Delta x/u_0.$$

In the case where Δt is chosen as the largest stable time step for advection, then we require $N \geq 1+1.4c_0/u_0$ for a stable dynamics timestep. Using a typical values $u_0 = 120\,\mathrm{m\,s^{-1}}$ and $c_0 = 340\,\mathrm{m\,s^{-1}}$ gives $N = 5$. CAM places additional restrictions on the time step (such as that the physics timestep must be an integer multiple of Δt), which also influence the choice of Δt and N. For a detail description of HOMME refer Taylor et al. (2008).

3 Results

The scales and periods of convectively coupled equatorial waves in the simulations are examined using the methodology of Wheeler and Kiladis (1999) (hereafter WK99). Figures 1 and 2 show symmetric and anti-symmetric components of the normalized power spectra of the outgoing longwave radiation (OLR) averaged from 15° S to 15° N from FV, EUL, and HOMME. This normalization procedure removes a large portion of the systematic biases within the models, and more clearly displays the model disturbances with respect to their own climatological variances at each scale. The regions of wavenumber-frequency space defining the

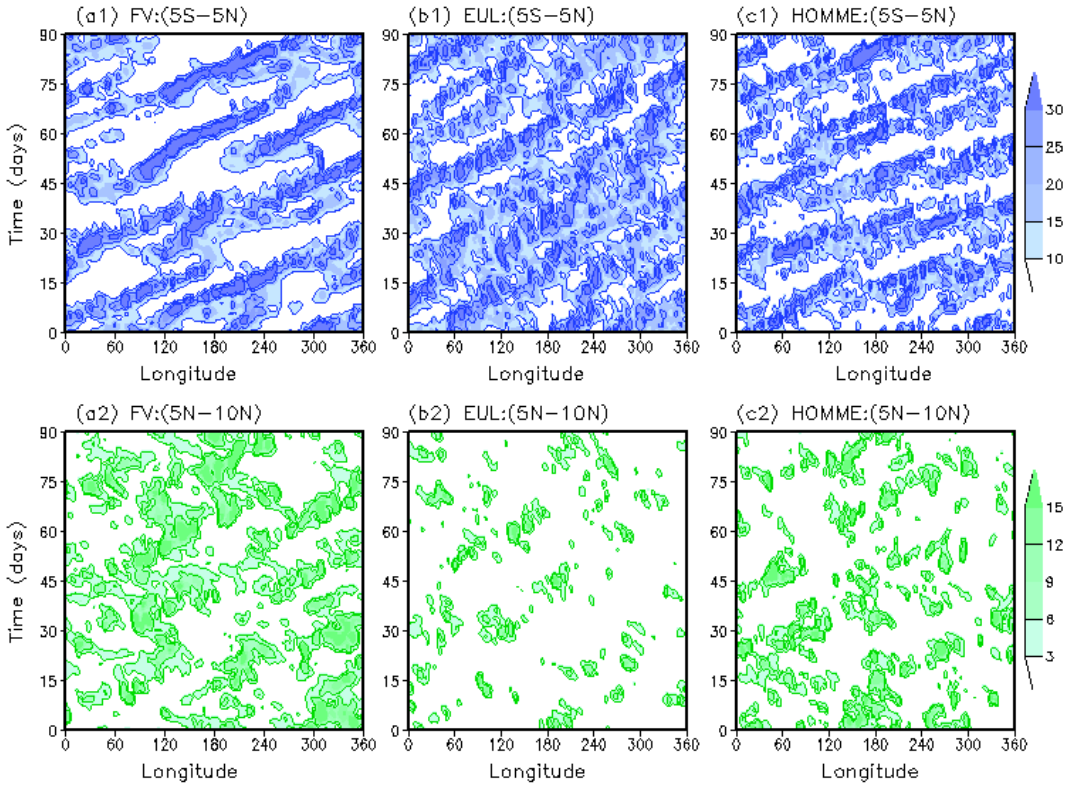

Fig. 3. Longitude-Time diagrams of surface reaching precipitation rates (mm/day) averaged between (top panel) 5° S–5° N and (bottom panel) 5° N–10° N from **(a1, a2)** FV, **(b1, b2)** EUL, and **(c1, c2)** HOMME.

(meridional mode $n = -1$) Kelvin, $n = 1$ equatorial Rossby (ER), $n = 0$ mixed Rossby-gravity (MRG), $n = 0$ eastward inertio-gravity (EIG), $n = 1$ westward inertio-gravity ($n = 1$ WIG), $n = 2$ westward inertio-gravity ($n = 2$ WIG) and Madden Julian Oscillation (MJO) modes are similar to WK99. The conventional dispersion curves of shallow water modes for equivalent depths of 12, 25, and 50 m are shown in the figures. The three dynamical cores show similar patterns: prominent Kelvin waves, but weak ER and MRG waves. This is not surprising since they use the same physics package. However, there exist some differences between them: speed of Kelvin waves, power in MJO, etcetera. We now discuss the notable differences and similarities between the three cases.

Inspection of Fig. 1 reveals that, in FV the Kelvin waves have most of their variance centered on an equivalent depth of approximately 12 m at lower wavenumber (<6), corresponding to a speed of 10.8 m s^{-1}. At higher wavenumbers (>6), the variance is centered on 25 m equivalent depth. In EUL there is a lack of power in Kelvin modes, especially at higher wave numbers (above 6). Similar to FV, at lower wavenumbers (below 6) the variance centered on 12 m equivalent depth, however at higher wavenumbers (above 6) most of the variance is at 50 m equivalent depth. The variance in HOMME centers around 25 m equivalent depth at lower wavenumbers, and centers around 50 m equivalent depth at higher wavenumbers, which is corresponding to 15.6 m s^{-1} and 22.1 m s^{-1}, respectively. Comparatively, HOMME does a better job in the simulation Kelvin waves with adequate variances and reasonable phase speeds similar to the observation (see Figs. 5 and 6 of WK99). In all the three simulations, there is an increase in the speed of Kelvin waves at smaller scales. The MJO is the other eastward propagating mode with period 30 to 70 days and wavenumbers 1 to 5. The symmetric component of the MJO is seen in Fig. 1. All the three dynamical cores show some variance within these bands. In FV, there are two spectral peaks; the primary one is between wavenumbers 1 and 3, and the secondary one at wavenumber 5. Similarly, EUL and HOMME have two spectral peaks. In EUL the primary peak is at wavenumber 5 and secondary peak between 1 and 2. On the contrary, HOMME shows two equally strong peaks, one between wavenumbers 4 and 5 and another between 1 and 3. Another notable point is that in EUL and HOMME there is an eastward propagation similar to the time scales of MJO, but at higher wavenumbers (above wavenumber 8), which is absent in FV. The symmetric component of the westward propagating disturbances in the wavenumber range of 1 to 10 and period from 10 to 20 days is the ER. It is seen from Fig. 1 that FV and EUL lack energy in this band, except around wavenumber 10. But in

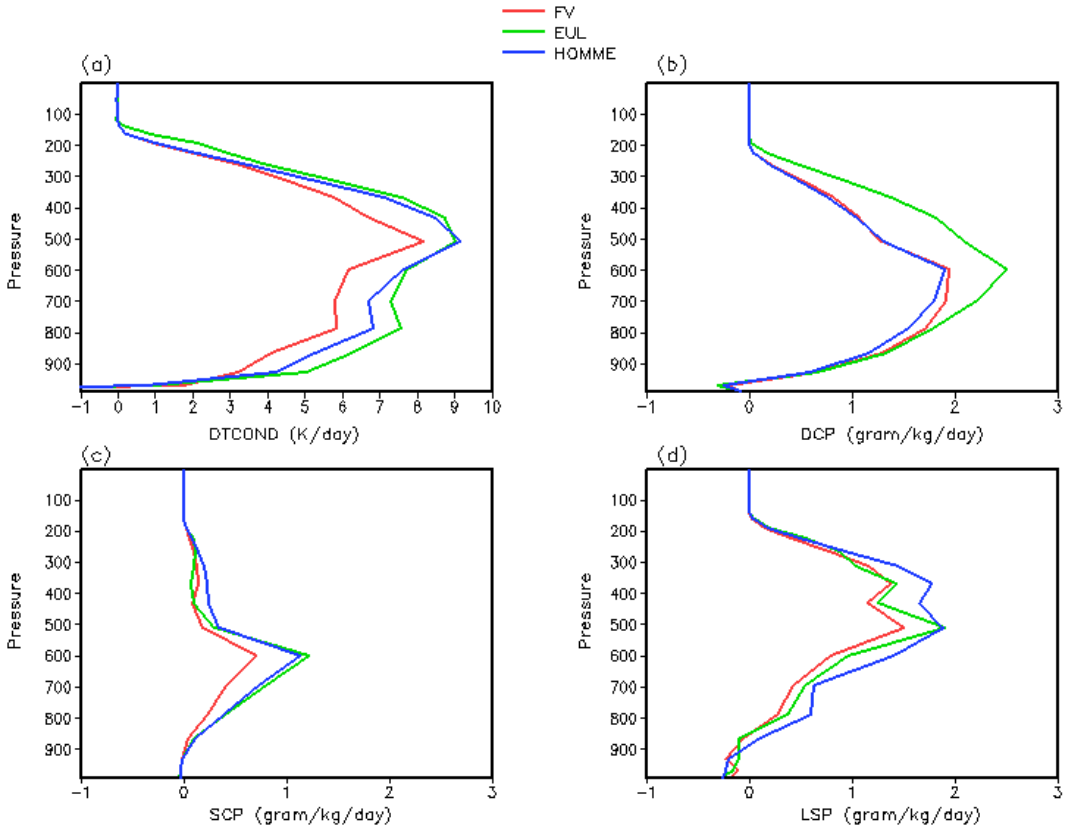

Fig. 4. Vertical distribution of **(a)** moist heating, **(b)** deep convective precipitation rate, **(c)** shallow convective precipitation rate, and **(d)** large scale precipitation rate in the deep tropics (0° E to 360° E and 2.5° S to 2.5° N) from FV, EUL, and HOMME.

HOMME, there is considerable amount of variance present in the smaller scales of this wave. The $n = 1$ WIG is another symmetric component of the westward propagating waves with less than 2.5 days time scale. In this regime, the variance is higher in HOMME than in the FV and least in EUL. Figure 2 shows the anti-symmetric waves. The variance in the MRG waves is very poor in all the three cases. In the EIG regime, the variances are weak, and phase speeds are too slow, scaled to shallow equivalent depths. However, relatively there is more variance in HOMME. The $n = 2$ WIG is weak in all the three dynamical cores (not shown here).

Figure 3 (top panel) presents longitude-time diagrams of precipitation rates near the equator (5° S–5° N), which forms the most active region for Kelvin waves and MJO. In all the three simulations, precipitation bands are moving eastward, resembling equatorial moist Kelvin waves (WK99). However there is a difference in the phase speed, with HOMME simulations being the fastest, followed by EUL, and slowest in FV. This is consistent with the results observed in wavenumber-frequency space. Secondly, the precipitation is found to be more organized in FV, whereas in EUL it appears in non-contiguous bands and indicates less organization. The organization in HOMME is better than EUL but not as coherent as that in FV. Similarly Fig. 3 (bottom panel) shows the same for the off-equatorial region, where most of the westward propagating disturbances occur. Since our model is hemispherically symmetric, we have shown only for Northern Hemisphere i.e. 5° N–10° N. A careful look at the details, however, reveals the small cluster propagating westward whereas the loosely grouped clusters propagate eastward in all the three simulations. However, in EUL, precipitation appears in patches with small values, while streaks of more intense and organized precipitation occur in FV and HOMME. In comparison precipitation is most organized in FV, with westward disturbances composed of the ER and MRG waves. We noticed in the wavenumber-frequency domain that ER is most prominent in HOMME and MRG is most prominent in FV. The longitude-time realization illustrates the same.

Since vertical structure of the moist heating is crucial in determining the speed of the eastward propagations, we have shown the same for the three dynamical cores in Fig. 4a, for the equatorial region (2.5° S–2.5° N). Comparison of FV and EUL indicates that throughout the troposphere, EUL has a greater heating rate than FV. The heating profile of HOMME largely falls in between the other two dynamical cores in the lower troposphere. However around 500 hPa, the heating in HOMME is closer to EUL and significantly more than that

in FV. Hence, comparatively, the top-heaviness in the heating profile is greater in HOMME than FV and EUL. In order to know the reason for the difference in the profile of the moist heating, the vertical distributions of the deep, shallow and large-scale precipitation rates are plotted in Fig. 4b, c, and d, respectively. It is noticed that there is a change in the partitioning between precipitation components. FV and HOMME have similar deep convective precipitation (DCP), less than that in EUL at all the model levels. On the other hand, shallow convective precipitation (SCP) is higher in EUL and HOMME than FV. The large-scale precipitation (LSP) is highest in HOMME, least in FV, and intermediate in EUL. The higher LSP in HOMME, especially in the upper troposphere, results in a more top heavy heating profile and is perhaps responsible for higher phase speed of the Kelvin waves.

4 Conclusions

The highly scalable dynamical core High Order Method Modeling Environment (HOMME) has been integrated into CAM4. Initial HOMME simulations have been completed in the aqua-planet configuration, using the CAM4 physics. The results of this simulation have been examined and the fidelity of HOMME in simulating equatorial waves, a crucial element of climate variability, was assessed. For this we compared the results from two other established dynamical cores of CAM4, the finite volume (FV) and Eulerian (EUL).

The principal features are similar across the three dynamical cores i.e. prominent Kelvin, weak $n = 1$ equatorial Rossby (ER), and feeble mixed Rossby-gravity (MRG) waves. However, important differences have been found. The phase speed of Kelvin waves in HOMME is faster and more reasonable than those in its counterparts. The higher phase speed is attributed to an increased large-scale precipitation in the upper troposphere and a more top-heavy heating structure. In the ER, $n = 1$ westward inertio-gravity (WIG), and $n = 0$ eastward inertio-gravity (EIG) regimes the variances are higher in HOMME than FV and EUL.

There are some biases common in all the three dynamical cores. The ER, MRG, and $n = 2$ WIG are too weak. There is an indication of an increased phase speed of Kelvin waves at smaller scales, whereas in the atmosphere the reverse does happen (see Figs. 5 and 6 of WK99). Since these are common in all three dynamical cores, the CAM4 physics may be a reason for the drawbacks.

All the three dynamical cores used the same physical parameterizations, which were originally developed and tuned for EUL and FV. To optimize the performance of HOMME, it will be necessary to re-adjust the parameterizations. Future work is to investigate the performance of HOMME in actual-planet framework and full tuning of the physical parameterization for HOMME to alleviate its shortcomings.

Acknowledgements. Many researchers have participated in the development of HOMME. We thank Amik St-Cyr, Jim Edwards, John Dennis, Jose Garcia, Michael Levy, Peter Lauritzen, Rich Loft, Rory Kelly, and Theron Voran for their contributions to HOMME development. Also thanks to Phil Rasch, and Sandeep Sahany for helpful discussions on the results presented here. Thanks are also due the referee and Paolo Michele Ruti (topical editor) for helpful suggestions. This work is supported by the US Department of Energy under grants DE-F402-07ER64464 and DOE/BER program DE-SC0001658. The National Center for Atmospheric Research is sponsored by the National Science Foundation.

Topical Editor P. M. Ruti thanks one anonymous referee for her/his help in evaluating this paper.

References

Bhanot, G., Dennis, J. M., Edwards, J., Grabowski, W., Gupta, M., Jordan, K., Loft, R. D., Sexton, J., St-Cyr, A., Thomas, S. J., Tufo, H. M., and Voran, T.: Early experiences with the 360TF IBM BlueGene/L platform, Int. J. Comput. Methods, 5, 237–253, 2008.

Canuto, C. G., Hussaini, M. Y., Quarteroni, A., and Zang, T. A.: Spectral Methods: Evolution to Complex GeometriesandApplicationstoFluidDynamics(ScientificCom-putation), Springer, 598 pp., 2007.

Dennis, J., Fournier, A., Spotz, W. F., St.-Cyr, A., Taylor, M. A., Thomas, S. J., and Tufo, H.: High Resolution Mesh Convergence Properties and Parallel Effciency of a Spectral Element Atmospheric Dynamical Core, Int. J. High Perf. Computing Appl., 19, 225–235, 2005.

Karniadakis, G. E. and Sherwin, S. J.: Spectral/Hp element methods for CFD, 408 pp., ISBN-13: 9780195102260, 1999.

Nair, R. D. and Tufo, H. M.: Petascale atmospheric general circulation models, SciDAC 2007, 24–28 June, Boston, USA, J. Phys. Conf. Ser., 78, 1–5, 2007.

Nair, R. D., Choi, H.-W., and Tufo, H. M.: Computational aspects of a scalable high-order discontinuous Galerkin atmospheric dynamical core, Comput. Fluids, 38, 309–319, 2009.

Neale, R. B. and Hoskins, B. J.: A standard test for AGCMs including their physical parameterizations. I: The proposal, Atmos. Sci. Lett., 1, 101–107, 2000.

Neale, R. B., Richter, J. H., Conley, A. J., Park, S., Lauritzen, P. H., Gettelman, A., Williamson, D. L., Rasch, P. J., Vavrus, S. J., Taylor, M. A., Collins, W. D., Zhang, M., and Lin, S.: Description of the NCAR Community Atmosphere Model (CAM4), Tech. Rep. NCAR/TN+STR, National Center for Atmospheric Research, Boulder, CO, 194 pp., available on-line at http://www.ccsm.ucar.edu/models/ccsm4.0/cam, 2010.

Taylor, M. A.: Conservation of mass and energy for the moist atmospheric primitive equation on unstructured grids, in Numerical Techniques for Global Atmospheric Models, Lecture Notes in Computational Science and Engineering, Springer, 363–384, 2010.

Taylor, M. A. and Fournier, A.: A compatible and conservative spectral element method on unstructured grids, J. Comput. Phys., 229, 5879–5895, 2010.

Taylor, M. A., Edwards, J., and St-Cyr, A.: Petascale atmosphere models for the community climate system model: a new develop-

ment and evaluation of scalable dynamical cores, J. Phys. Conf. Ser., 125, 1–10, 2008.

Taylor, M. A., Edwards, J., Thomas, S., and Nair, R.: A mass and energy conserving spectral element atmospheric dynamical core on the cubed-sphere grid, J. Phys. Conf. Ser., 78, doi:10.1088/1742-6596/78/1/012074, 2007.

Wheeler, M. and Kiladis, G. N.: Convectively coupled equatorial waves: Analysis of clouds and temperature in the wavenumber-frequency domain, J. Atmos. Sci., 56, 374–399, 1999.